Modeling and Verification of Error Propagation in Integrated Additive/Subtractive Multi-Directional Direct Manufacturing

Rajeev Dwivedi, Srdja Zekovic, Radovan Kovacevic
Research Center for Advanced Manufacturing
Southern Methodist University, 3101 Dyer Street
Dallas TX- 75205

Reviewed, accepted September 14, 2006

Abstract

Integrated additive-subtractive manufacturing, when applied in the framework of Solid-Freeform-Fabrication (SFF) allows the fabrication of functional parts on single platform, directly from its computer model. Reduction in process complexity and total processing steps is ensured by multi-directional material deposition and machining. However, due to shift in the datum location in reorientation steps and sequential addition of material in the form of layers, the CAD process intent is not exactly replicated. This leads to inclusion of dimensional errors. Machining in order to eliminate the errors as frequent as layer deposition is highly expensive and can be avoided by estimation of errors and varying process parameters, and/or performing machining after a set of layers are deposited. This paper proposes a state space model for modeling the error propagation due to linear as well as angular variation in the datum. The model is based on identification of possible sources of error, mechanism of error inclusion and influence of process parameters. An experiment performed to determine parameters of error modeling has been reported.

1 Introduction

Inherent to most of the SFF methods is limited replication of CAD process model on the fabricated part. While designer's intent can be perfectly captured in the CAD model of a part, it is relatively difficult to implement it in the SFF. The reasons include limitation of spatial manipulators and the parameters associated with the mode of material delivery. A near perfect geometry can be obtained by control of process parameters; however, human intervention and post-processing in order to get the finished part is inevitable. Common to most of the material deposition techniques for SFF methods is energy enabled phase transformation. This phenomena leads to inclusion of errors in the dimensions and tolerances of the final part. Since SFF is a sequential process, addition of a layer takes place on the previously deposited layers. This leads to cumulative addition and propagation of errors. For the initial layers the deviation introduced is not pronounced; however, as the number of layers increases, the accumulation of deviations leads to a large difference between the desired and the actual build up height. The layer based deposition has certain issues inherent to it such as:

1. The deviation in the final dimension is a cumulation of the deviation along each layer.
2. The measurement of deviation for every layer is time consuming and requires lot of human intervention.

3. The process is comprised of discrete sub-tasks arranged in a sequential manner therefore is complex.

The likelihood of errors increases as the complexity of the spatial manipulation increases i.e. multi-directional deposition for SFF. For the multi-directional deposition, the geometry obtained in intermediate steps is transformed in the space. The transformations include linear, rotary or a combination of two. In general, for a $2\frac{1}{2}$ deposition approach, the process model assumes that the top surface generated by the deposition is flat.

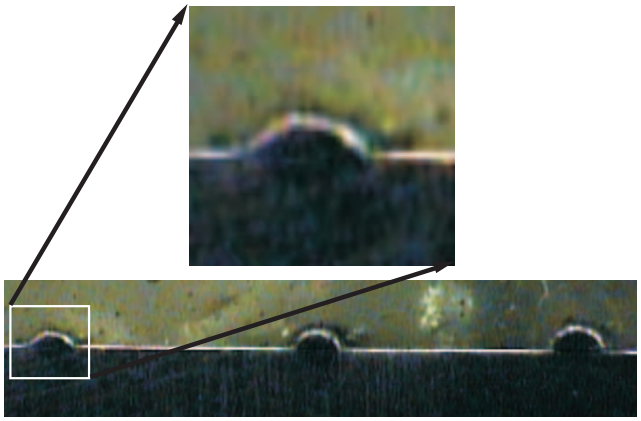

Fig. 1: Typical Bead Profile for different Process Parameteres (Power = 250, 300, 400 W)

For the layer based methods such as the Laser-Cladding, Gas Metal Arc Welding, and Gas Tungsten Arc Welding, the metal addition is done by generating a molten pool and adding the raw material in the form of wire or powder to the molten pool. The generated beads are not square. The amount of material along the bead profile changes. Fig. 1 shows the bead profiles obtained for a set of process parameters. The amount of material changes with respect to the distance from the center. Near uniformity of the top surface of the layer is obtained by overlapping the beads; however, the deviation from the desired profile cannot be completely eliminated. On the contrary, along the lateral direction the same is difficult to implement. The material addition is limited by the flow and direction of material delivery.

In the multi-directional deposition the lateral face of the manufactured geometry offers datum for fabrication of various features. Therefore the geometry of lateral profile of the layer becomes extremely important. Due to limitation of the methods, the control of lateral profile geometry becomes challenging. The usual method of overlapping the adjacent beads can be applied partially.

One of the widely used approaches to get a planar deposition profile includes machining at the intermediate level [1–4] . The disadvantages that can be associated with the approach include :

1. Wastage of material.

2. Slower process.

The estimation, modeling, and optimization of the errors in rapid prototyping has been analyzed in the references [5–8]; however, the methods primarily address the variation due to the stair-case effect introduced in the process. Charney et. al. [9] suggest a quantitative model of tolerances and part geometry in relation to the process variables. The surface profile and the subsequent errors

play a very important role in the geometry of the final part; however, the published results offer very limited inputs for the process improvement [10].

This paper proposes the state space model of SFF based part fabrication and error by depositing material along multiple directions. Model estimates the geometry of deviation and the pattern of deviation accumulation. The model focuses on the Laser-based deposition; however, it can be applied to other methods of metal deposition such as Welding- and Plasma-based metal deposition. Using the model the geometry of deposition profile can be determined. Using the inputs from deposition profile, the process parameters can then be adjusted to obtain a smoother geometry and reduce the overall deviation in the part geometry.

The initial part of the paper suggests the model for part fabrication by sequential layered deposition in a $2\frac{1}{2}$ and multi-directional framework. Next, the sources of deviation are identified and a quantitative model of the process and the model of geometric reconstruction by depositing metal is suggested. The model then is extended towards exclusive derivation of deviation geometry. Finally, quantified cumulative effect of error propagation is expressed. The paper concludes with description of an experiment for the determination of error model parameters.

2 SFF based on multi-directional deposition

The framework of can be classified as -"divide and conquer". Any solid is approximated as a set of stacked layers such that, the solid fabricated by the SFF exhibits a near uniform cross-section over each layer. The geometry of a layer is expressed by area A and swept along the vector $\hat{v_g}$ where the subscript g corresponds to the growth direction. The final geometry is the cumulative integration of the set of individual layers expressed as:

$$P = \bigcup_{i=1}^{n} A_i \oplus \hat{v_g} \tag{1}$$

where $\oplus$ represents the Minkowski sum and $A_i \oplus \hat{v_g}$ is the translation of i^{th} cross-section A_i along the vector $\hat{v_g}$.

For a multidirectional deposition the growth direction vector is different for different regions, therefore the above model is expressed as:

$$P_{multi-direction} = \bigcup_{i=1}^{n} \bigcup_{j=1}^{m} A_j \oplus \hat{v_i} \tag{2}$$

where the variables m and n correspond to the number of layers and the number of regions with distinct growth vectors respectively.

3 Modeling the error in SFF based on multi-directional deposition

Contrary to the ideal model for SFF, in the actual implementation scenario, errors are inducted due to limited control of the process parameters. The actual profile of the layer has two different components, the desired profile and the profile of geometrical error of a layer expressed as:

$$p_a = p_d \oplus err(p_d) \tag{3}$$

where p_a is the actual layer profile, p_d is the desired profile and $err(p_d)$ is the error introduced during deposition of the layer. Correspondingly the actual profile of geometry obtained by sequential deposition of layers has two different components, the desired geometry and the profile of accumulated geometrical errors expressed as:

$$P_d \oplus err(P_d) = \bigcup_{i=1}^{n} p_d \oplus err(p_d) \tag{4}$$

where, P_d is the desired cumulative profile and $err(P_d)$ is the cumulative error introduced during deposition of n layers. Due to fundamental nature of the deposition, the error can be self adjusting, that is surplus material in one stage may be compensated by material deficit in further stages and vice versa. With the self adjusting nature of the material deposition, measures such as machining may be completely eliminated or introduced with lesser frequency.

Many existing SFF methods are based on $2\frac{1}{2}$ axis deposition. Other methods such as SLA and SLS allow multi-directional deposition; however, the requirement of support is not completely eliminated. Fabrication of support structures for the overhanging regions is one of the primary limitations. Alternatively multi-directional deposition may be used to fabricate parts having overhanging regions. Multi-directional deposition is enabled by determining the morphology of the overhanging region, then determining the orientation vector and finally reorienting the substrate or the pre-deposited material in the space to generate a datum. The datum generated for the new configuration thus allows material deposition for the sub-regions without support requirement. A detailed discussion on the process planning for multi-directional deposition is beyond the scope of this paper. However authors would like to suggest a set of previous papers [11–13] for more information.

Inherent to the transform of datum is the spatial transform of layer profile. The transformed profile is expressed as:

$$l_d = t.(p_d \oplus err(p_d)) \tag{5}$$

where l_d is the transformed profile of the layer and t is the transformation matrix. Correspondingly the cumulative transformed profile is expressed as:

$$L_d = T.\bigcup_{i=1}^{n}(p_d \oplus err(p_d)) \tag{6}$$

where L_d is cumulative geometry and T is the cumulative transformation matrix. On transforming the datum used to manufacture a sub-region the overall profile of the sub-region is transformed. The transformation is expressed as:

$$P = (T.L) \oplus (\bigcup_{i=1}^{n} p_d \oplus err(p_d)) \tag{7}$$

where L is the profile of the datum on which sub-region is built. A close observation suggests that the error depends on the datum and the immediate process errors introduced during the deposition.

Contrary to the machining and other modes of fabrication, the geometry obtained by SFF is governed by the zig-zag pattern of relative motion in a plane. Complex features with non-linear geometry such as fillets and circular holes are obtained by the manipulation of the zig-zag path. Due to the mode of material addition, the pattern of excess and deficit material is different along

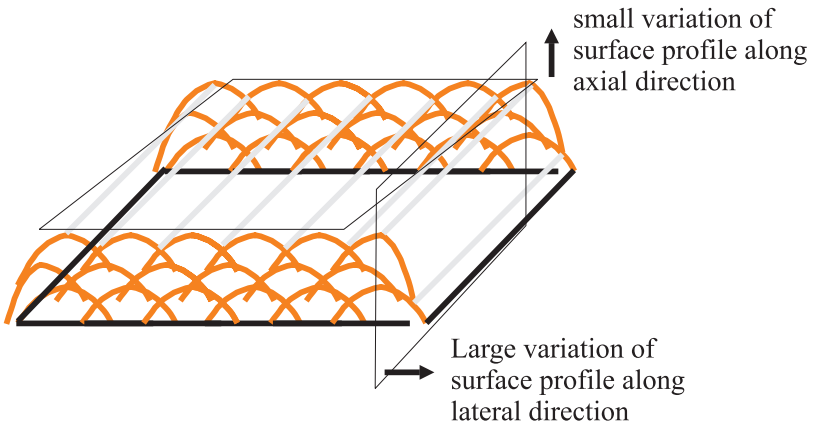

Fig. 2: Variation of surface profile along the axial and lateral directions of bead deposited geometry

the different directions. Also, the deficit or excess of material along the different directions is independent with respect to each other (Fig. 2).

For the deposition along z-direction, suitable overlap allows generation of near flat top profile. A model of error estimation along the z-direction for $2\frac{1}{2}$ deposition has been suggested by the authors in [14]. Along the lateral direction however ($x-y-$ plane) the overlap does not allow compensation and subsequent smoother profile. The uneveness along the outer profile is characteristic of the deposition parameters and therefore estimated directly (Fig. 2). Before a surface is established as datum and further deposition performed, it must be machined. Machining on a surface is required before the surface is established as the surface of final part.

4 State space model of deviation propagation

The process planning in all of the SFF techniques starts with the CAD model of the object. For multi-directional deposition the solid is decomposed into a set of subregions, based on the requirements of supporting structures. Next, a suitable growth direction for every subregion is defined and the subregion is sliced along the growth direction by a set of parallel planes. The slicing in essence generates a set of 2D contour geometry. A suitable path is generated to fill the 2D contour area. The metal deposition head sweeps along the path to fill the material in the area. The 2D contour area generation and the sweeping is performed for all the layers in a suitable sequence to fabricate the part. Two most important factors that determine the accuracy of the part geometry are: (1) the accuracy of the layer geometry and the accuracy of cumulated layer geometry, and (2) how accurate the datum is established.

SFF region model (Fig. 3): Each multi-directional region is uniquely defined by the location of its datum $s : \vec{s_d} = [x_d, y_d, z_d]^T$, the orientation vector for the growth of region $v : \vec{v_g} = [n_x, n_y, n_z]^T$ and the set of desired cross-sectional profile of the layers $Sc : [c_1(p,q,r) = 0, c_2(p,q,r) = 0, \ldots, c_n(p,q,r) = 0]$. The p, q and r are the local coordinate system along the plane of a layer. Therefore, the set that captures the minimum set of parameters required to describe a region is $Pr = \{s, v, Sc\}$. A part comprised of n different regions can be described by the region set expressed as:

$$P = \{Pr_1, Pr_2, \ldots Pr_n\} \tag{8}$$

Therefore any region i is expressed as:

$$R_i = [(x_d)_i, (y_d)_i, (z_d)_i, (n_x)_i, (n_y)_i, (n_z)_i, \\ (c_1(p,q,r))_i, (c_2(p,q,r))_i, \ldots, (c_n(p,q,r))_i]^T \tag{9}$$

Correspondingly the part is represented as :

$$P = [R_1, R_2, \ldots R_n]^T \tag{10}$$

Geometric deviation: The deviation along the datum location of subregion, orientation vectors and the cross-sectional profiles of every subregion characterize the overall deviation in the part expressed as:

$$\triangle R_i = [(\triangle x_d)_i, (\triangle y_d)_i, (\triangle z_d)_i, (\triangle n_x)_i, (\triangle n_y)_i, (\triangle n_z)_i, (\triangle c_1(e_x, e_y, e_z))_i, \\ (\triangle c_2(e_x, e_y, e_z))_i, \ldots, (\triangle c_n(e_x, e_y, e_z))_i]^T \tag{11}$$

Determination of geometric deviation: The correlation between the overall geometry of the solid and the parameters of the subregions of the solid can be captured by a linearization based on first-order differential equation:

$$\triangle P_i = \frac{\partial}{\partial R} f(R) \triangle R + res \tag{12}$$

where the function f correlates the part geometry P to the geometric parameters of different subregions of the solid. res is the residual for linearization treated as noise. Attributing a parameter that corresponds to various stages of SFF based part fabrication that is (1) deposition for a layer and, (2) reorienting and redefining the datum, the process can be expressed by a state-space equation for discrete continuous time variant system described as:

$$y(t) = C(t)x(t) + d(t) \tag{13}$$

where t is the time equivalent for a step. $y = \triangle P_i$, $C(t) = \frac{\partial}{\partial R} f(R)$. In a sequential SFF process the deposition of a layer is performed on a substrate or previously deposited layers. The sequential addition of material and corresponding geometry is expressed by:

$$x(t+1) = A(t)x(t) + b(t)u(t) + w(t) \tag{14}$$

where $A(t)$ is measures the deviation of a layer that is deposited on the datum established by previous layer. $B(t)u(t)$ is the deviation introduced by difference in the datum location and possible errors in relative motion of the metal deposition head. $w(t)$ is the system noise. The state equation is based on the assumption that the surface used as the datum for deposition has been machined to remove possible excess of material. Incorporation of the error induction in the intermediate stages of machining can be done in the suggested framework; however, it does not lie in the scope of this work.

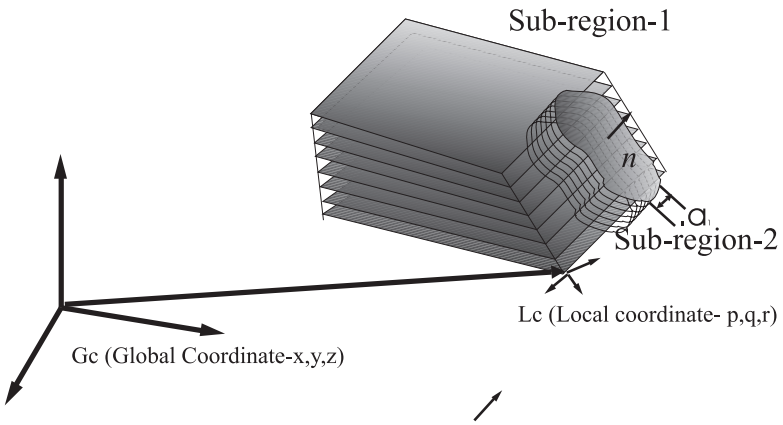

Fig. 3: The Coordinate Systems used in the Error Propagation Estimation

5 Modeling the surface profile

The modeling of the process is determined in two coordinate systems (Fig. 3). The first coordinate system is the global coordinate system (G_c) and is attached to the substrate; whereas the second coordinate system is attributed to the immediate surface used for deposition (L_c). The change in dimensions due to temperature rise is ignored and, therefore, the location and orientation of the G_c is ignored as well. L_c, however, changes as each layer is deposited.

The desired shape of the object is characterized by the final axial-coordinates of various points along the top layer of different sub-regions. The deviation of the axial-coordinate in the k^{th} layer can be expressed by the following relationship:

$$^{R}A_k(x,y,z) = T(\theta,\phi,\triangle x_c,\triangle y_c,\triangle z_c)\sum_{i=1}^{k} a_i(p,q) \tag{15}$$

where $^{R}A_k(x,y,z)$ is the geometry of k^{th} layer profile of the sub-region R as observed in the global coordinate system. $\theta,\phi,\triangle x_c,\triangle y_c,\triangle z_c$ are the parameters of the local coordiante system of immediate layer. T is the transformation matrix that connects the global coordinate system to the local coordinate ystem. a_i is the contribution to thickness in the i^{th} layer. The deposition, therefore, can be characterized by the set of thicknesses for each layer expressed as:

$$A_k(x,y,z) = [\theta,\phi,\triangle x_c,\triangle y_c,\triangle z_c,a_1,a_2,\ldots,a_k] \tag{16}$$

The behavior of the error propagation is assumed to be monotone; however, depending upon the geometry and the process parameters, the machining in an intermediate stage becomes inevitable. For such cases, the method suggested in this paper can be introduced between two stages of machining.

Any arbitrary surface is characterized by an infinite number of points; therefore, we focus on a representative set of points for the diagnosis and the measurements. The total number of points may vary for different geometries. The formulation of the deviation propagation is based on a state space model. As described in Fig. 4 the deviation for a given layer is the result of :

1. The error introduced during the deposition of the layer.

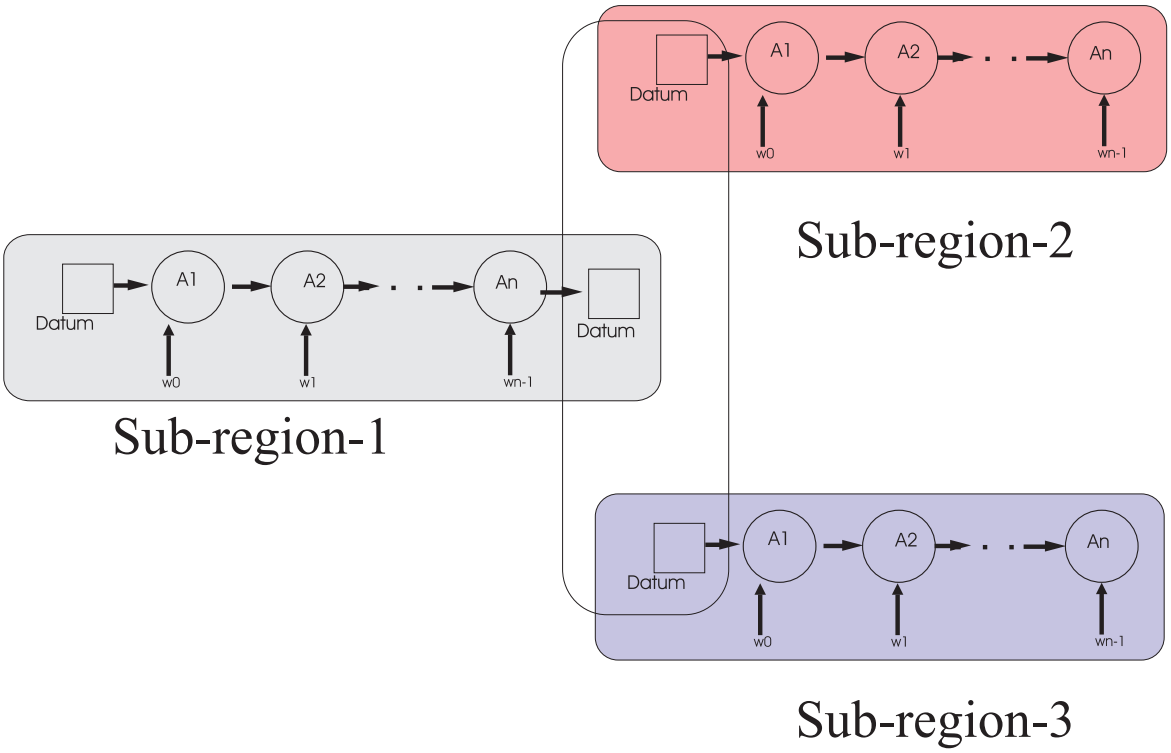

Fig. 4: The Model of Error Accumulation

2. The accumulation of errors due to deposition along the previous layers.

3. Error in the datum.

The deviation in the top profile of the deposition is, therefore, expressed by the following relationship:

$$\tilde{A}_k(x,y,z) = \tilde{A}_{k-1}(x,y,z) + \tilde{F}_{k-1}(x,y,z)\tilde{w}_{k-1}(x,y,z) \tag{17}$$

where $\tilde{Z}_k(x,y)$ is the deviation in the height and orientation of the k^{th} layer at the location (x,y). $\tilde{w}_{k-1}(x,y)$ is the variation associated with the deposition of the layer $k-1$, and the $\tilde{F}_{k-1}(x,y)$ matrix transforms the variation in the layer $k-1$ with respect to the substrate. By introducing another equation:

$$S_k(x,y,z) = \tilde{A}_k(x,y,z) \tag{18}$$

the deposition process can be represented to be in a state-space form [15] with Eq. 17 and Eq. 18 representing the state and the output equations, respectively.

One of the assumptions that can be made towards the suitable treatment of the errors is that, the variation $\tilde{w}_k(x,y,z)$ is a normally distributed random variable. Further, a suitable distribution function could be attributed to the random variable.

6 A model for material addition in SFF based on Laser deposition

As described earlier, the deposition for most of the SFF techniques does not allow a uniform profile and the amount of material varies in space. The near planar surface profile can be obtained by overlapping two beads.

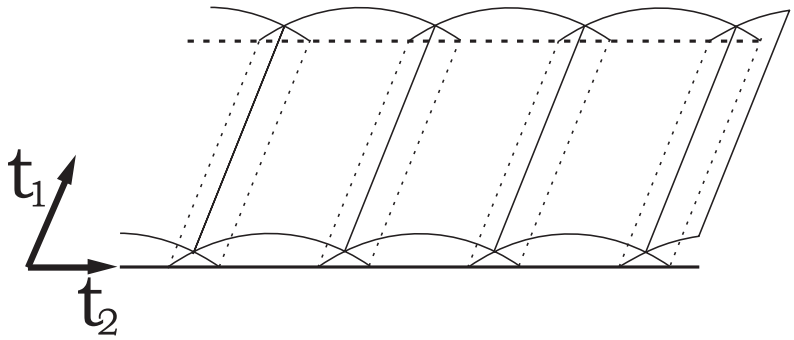

Fig. 5: Material deposition defined by the directions t_1 and t_2

One of the important factors in the overlap is the selection of the phase difference between the two adjacent beads. Let the function $f(t_1, t_2)$ represent the cross-section profile of the bead (Fig. 5); t_1 and t_2 define the datum plane of the layer onto which the deposition is done; then for two beads separated by the vector $\triangle t_1 \hat{e_1} + \triangle t_2 \hat{e_2}$, the cumulative profile is expressed by:

$$F(t_1, t_2) = f(t_1, t_2) + f(t_1 + \triangle t_1, t_2 + \triangle t_2) \tag{19}$$

However, due to the zig-zag pattern of deposition, the variation along t_1 is negligible; therefore, the degrees of freedom of the system can be reduced to:

$$F(t_1, t_2) = f(t_1, 0) + f(t_1 + \triangle t_1, 0) \tag{20}$$

The deposition is performed in sequential fashion with equally spaced layers. Hence, the profile obtained after deposition of n layers is expressed by:

$$F_n(t_1, t_2) = n(f(t_1, 0) + f(t_1 + \triangle t_1, 0)) \tag{21}$$

When observed in the global coordinate system, the corresponding profile is expressed by:

$$^nF_G(x, y, z) = T(\theta, \phi, \triangle x_c, \triangle y_c, \triangle z_c) F_n(t_1, t_2) \tag{22}$$

Observations (Fig. 6 and Fig. 1) suggest that, for a wide range of process parameters, the bead-profile in the laser-based deposition can be approximated as a sinusoid. The cumulative profile representation of the deposition can be represented by a specific form of Eq. 21 expressed as:

$$Z(x) = C \sin(\frac{\pi x}{Bw}) \;\; such \;\; that \;\; 0 \leq x \leq Bw \tag{23}$$

where Bw is the total width of the bead. C is a suitable constant corresponding to the geometry of the bead. The overlap of two beads can be expressed by the following relationship:

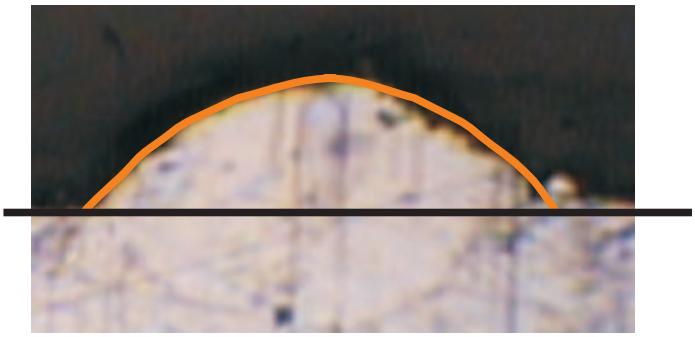

Fig. 6: Sinusoidal approximation of the bead profile

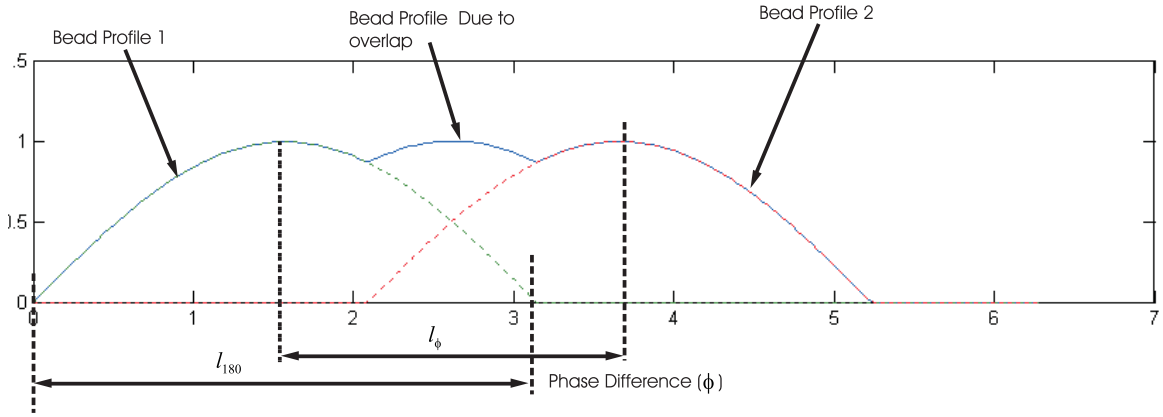

Fig. 7: The optimal profile obtained by overlapping two beads

$$Z_{overlapped}(x) = C(\sin(\frac{\pi x}{Bw}) + \sin(\frac{\pi x}{Bw} + \frac{\pi l}{Bw})) \tag{24}$$

where l represents the separation between two overlapping beads. A suitable value of the l can be determined to get a smooth top profile (Fig. 7). The deposition over an inclined surface can be modeled as the skewed transform of the bead profile for horizontal surface (Fig. 8) expressed as:

$$Z_{inclined-overlapped}(x) = Skew(C(\sin(\frac{\pi x}{Bw}) + \sin(\frac{\pi x}{Bw} + \frac{\pi l}{Bw}))) \tag{25}$$

where $Skew()$ is the skew transformation function along $x - axis$. For the laser-based metal deposition the surface tension of the molten metal and rapid solidification allow a negligible variation in the profile obtained by overlap. In the actual process implementation, the overlapping of the beads allows the remelting of previously deposited layer and hence a smoother surface; however, it is difficult to get a flat top surface. The cumulative overlap of multiple beads allows a near smooth deposition.

6.1 Modeling of layer profile and its variation

For most of the metal deposition techniques, the deposition follows a zig-zag pattern or variants of the zig-zag pattern.

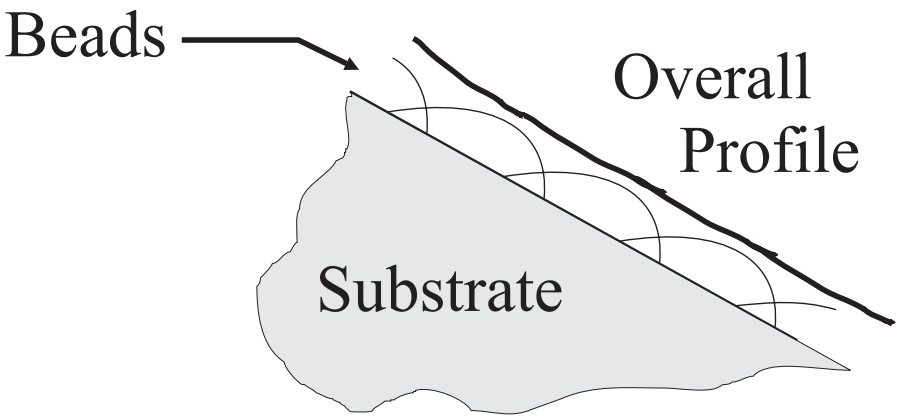

Fig. 8: Profile of beads along incline obtained as skew transform of horizontal bead profiles

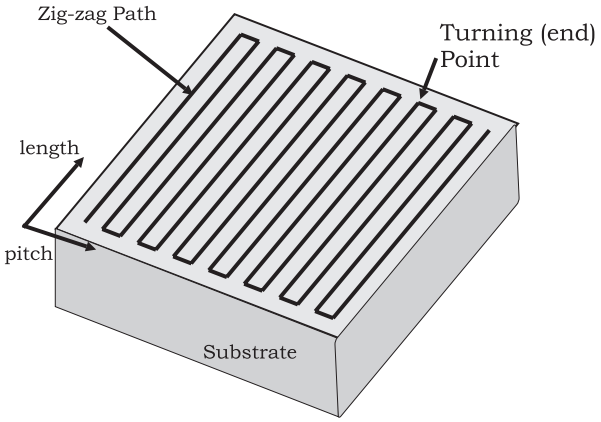

Fig. 9: A Cross-sectional area and the corresponding zig-zag path

The zig-zag pattern is characterized by a set of interconnected parallel line segments as shown in the Fig. 9. In order to simplify the modeling of deposition the turning effects along the end of the path segments is ignored. The distance between the parallel lines is characterized by the extent of overlap between two path segments that in turn depends on various process parameters. A 2D coordinate system is attributed to characterize the path pattern. The first coordinate axis is directed along the length of the path; whereas, the other coordinate axis is directed along the pitch of the path. The profile of the deposition about a given length of the path is, therefore, expressed by:

$$Z_n(x) = \sum_{i=1}^{n} Skew(C_i(\sin(\frac{\pi\ modulo(\frac{x}{2l_i})}{Bw_i}) + \sin(\frac{\pi\ modulo(\frac{x}{2l_i})}{Bw_i} + \frac{\pi l_i}{Bw_i}))) \tag{26}$$

where n is the maximum number of layers, x is the location of the path segment, l_i is the distance between two consecutive beads, and $modulo()$ is the 'modulo' or the 'remainder' function. The variation of profile therefore, in the deposition can be modeled as:

$$\tilde{Z}_n(x) = f_1(\sum_{i=1}^{n-1} Skew(C_i(\sin(\frac{\pi\ modulo(\frac{x}{2l_i})}{Bw_i}) + \sin(\frac{\pi\ modulo(\frac{x}{2l_i})}{Bw_i} + \frac{\pi l_i}{Bw_i})))) + \\ F_{n-1}(x) f_2 Skew((C_n(\sin(\frac{\pi x}{Bw_n}) + \sin(\frac{\pi x}{Bw_n} + \frac{\pi l_n}{Bw_n})))) + err(n) \tag{27}$$

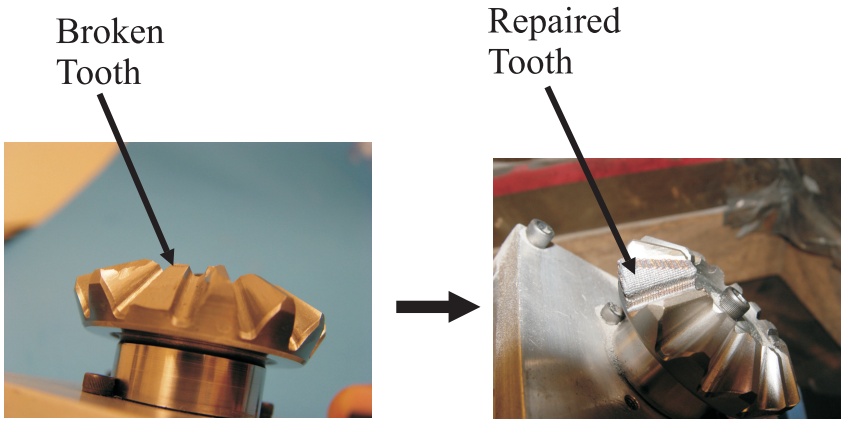

Fig. 10: Repaired Part. The part offers an inclined face of 30^o

The functions $f_1()$ and $f_2()$ described in Eq. 27 capture the influence of the remelting during the deposition and function $err()$ captures the random errors. However, modeling the functions $f_1()$, $f_2()$ and $err()$ is not trivial due to the involvement of a wide range of process parameters and other variables such as the influence of the underlying substrate geometry. A set of experiments and observations are performed to arrive at a model for the horizontal datum and are reported in [14]. We perform a set of experiments for a face inclined at 30^o with respect to the horizontal axis. Repair of the damaged teeth of a bevel gear was chosen for the experiment. The damaged teeth was machined to generate a planar face inclined at 30^o as shown in Fig. 10. The allowable limit of the deviation is of the order of 0.2 mm. Whereas the limit of deviation for the inclination is 1^o. Once the limit for the deviation exceeds the suggested limit, the top surface is faced off and prepared for further deposition.

7 Experiments and the Observation

Parameter	**Value**
Power	200 W
Torch Speed	5 mm/s
Phase Difference	$\frac{2\pi}{3}$
Gas Flow	0.0354 m^3/hr
Layer thickness	0.4 mm
Path pattern of alternate layers	offset

Table 1: The process parameters used for the experiments

The experimental results used for the analysis are based on the set of process parameters described in the Table 1. Since the skew transform is a linear transform we can assume that the value corresponding to the phase difference of $\frac{2\pi}{3}$ between the adjacent beads, as obtained for the horizontal beads (Fig. 7) when applied for inclined beads gives near horizontal profile. A comparison of the measured surface profile and the profile in the CAD model is done. Of primary concern is the deficit of material due to deviation. The excess material can be removed by machining in the post processing operation; however, adding material for the deviations leading to deficit is extremely complex, therefore is avoided. The experiment is performed and the measurements are done for every layer. The total number of layers is recorded (NL_{max}) before the deficit is observed. Also, the number of layers is stored before the positive deviation exceeds 0.2 mm (ND_{max}). The maximum layers $N\theta_{max}$ before which allowable positive or negative angular deviation 1^o appears is stored. The values obtained for the experiment are:

- $NL_{max} = 8$,
- ND_{max} = excess did not appear.
- $N\theta_{max}$ = no angular deviation observed.
- maximum deviation value = -0.25mm

A set of measurements, for the experiments performed, provide the following set of functions for the model:

$$f_1(n) = f_2(n) = 1.4nh(1 - 0.20\lfloor\frac{n}{2}\rfloor) \quad 2 \leq n \leq 7 \tag{28}$$

where h is the maximum bead height. The functions $f_1()$ and $f_2()$ may vary for different set of process parameters. The sequential deposition for more than 7 layers introduces deficit and, hence, deviation in the surface profile.

8 Conclusions

A model of the origin of geometrical error and propagation of errors in the SFF based part fabrication was developed. The model includes linear as well as angular deviations in the geometry of the subregions and the overall geometry of a part. An experiment is performed to determine the parametric equation. A range of experiments should be performed to develop a more general parametric equation for the angular deviations.

Acknowledgments

This work was financially supported by the National Science Foundation Grants No. DMI-0320663 and DMI-0541952. Authors would like to acknowledge the help from Mr. Michael Valant Research Engineer, Research Centre for Advanced Manufacturing.

References

[1] F. W. Liou, J. Choi, R. G. Landers, V. Janardhan, S. N. Balakrishnan, and S. Agarwal. Research and development of a hybrid rapid manufacturing process. In *Proceedings of* 12^{th} *Solid Freeform Fabrication Symposium*, pages 138–145, University of Texas, Austin, August 2001.

[2] Zoran Jandric. *Optimization of Hybrid Rapid Manufacturing/Repair Process*. PhD thesis, Southern Methodist University, Department of Mechanical Engineering, May 2003.

[3] Radovan Kovacevic. Will we use welding technology to make rapid prototypes. *SME's Manufacturing Engineering Magazine*, (4):26–27, 2001.

[4] K. Hartman, R. Krishman, R. Merz, Gennady Neplotnik, Fritz B Prinz, Lawrence Schultz, M. Terk, and Lee Weiss. Robot-assisted shape deposition manufacturing. In *Proceedings of the 1994 IEEE International Conference on Robotics and Automation (ICRA '94)*, volume 4, pages 2890 – 2895, May 1994.

[5] Georges M Fadel and Chuck Kirschman. Accuracy issues in cad to rp translations. *Rapid Prototyping Journal*, 2(2):4–17, 1996.

[6] S. H. Choi and S. Samavedam. Modelling and optimisation of rapid prototyping. *Computers in Industry*, 47(1):39–53, 2002.

[7] F. Lin, W. Sun, and Y. Yan. A decomposition-accumulation model for layered manufacturing fabrication. *Rapid Prototyping Journal*, 7(1):24–31, 2001.

[8] Ramakrishna Arni and S. K. Gupta. Manufacturability analysis of flatness tolerances in solid freeform fabrication. *Journal of Mechanical Design*.

[9] Charity Lynn-Charney and David W Rosen. Usage of accuracy models in stereolithography process planning. *Rapid Prototyping Journal*, 6(2):77–87, 2000.

[10] R. Kovacevic, R. Mohan, M. Murugesan, and A. Seybert. On-line monitoring of the electric arc spraying process based on acoustic signatures. *Journal of Engineering Manufacture*, 209:369–379, 1995.

[11] R. Dwivedi and R. Kovacevic. An expert system for generation of machine inputs for laser-based multi-directional metal deposition. *Accepted for publication by International Journal of Mechanical Engineering Science*, October 2005.

[12] R. Dwivedi and R. Kovacevic. Process planning for multi-directional laser-based direct metal deposition. *Proceedings of the I MECH E Part C Journal of Mechanical Engineering Science*, 219(7):695–707, July 2005.

[13] R. Dwivedi and R. Kovacevic. Process planning for solid freeform fabrication based on laser-additive multi-axis deposition. In *Proceedings of the fourtheenth Solid Freeform Fabrication symposium*, pages 1–12, Austin, TX, August 4-6 2003.

[14] R. Dwivedi, S. Zekovic, and R. Kovacevic. A model for error propagation in the solid freeform fabrication. In *Proceedings of the sixteenth Solid Freeform Fabrication symposium*, Austin, TX, August 1-3 2005.

[15] Katsuhiko Ogata. *Modern control engineering (3rd ed.)*. Prentice-Hall, Inc., Upper Saddle River, NJ, USA, 1997.